PRECAST HYBRID MOMENT FRAME FUNCTIONAL RECOVERY PREQUALIFICATION

Final Report Submitted to the PUC (1/5/2026) for Consideration in the 2026 NEHRP Provisions

FUNCTIONAL RECOVERY PREQUALIFICATION REPORT FOR PRECAST HYBRID MOMENT FRAMES

Final Report Submitted to the PUC for Consideration in the 2026 NEHRP Provisions

Prepared By:

Resilient Design Coalition

Financially Supported by:

Clark Pacific and the Charles Pankow Foundation

TECHNICAL WORK AND AUTHORSHIP BY:

Ed Almeter, MS
Kristen Blowes, PhD, PE
Jared DeBock, PhD, PE
Curt Haselton, PhD, PE
Carlos Molina Hutt, PhD, PE
Huy Pham, PhD
David Welch, PhD
Reid Zimmerman, SE

January 5, 2026

QUANTIFICATION OF FUNCTIONAL RECOVERY SEISMIC PERFORMANCE FACTORS FOR PRECAST HYBRID MOMENT FRAMES

Submitted: 01/05/2026

EXECUTIVE SUMMARY

A quantification of the functional recovery seismic performance factors for the Precast Hybrid Moment Frame (PHMF) lateral force resisting system is performed in accordance with the proposed Section A.8.3.6 procedures in Appendix A of the 2026 National Earthquake Hazards Reduction Program (NEHRP) Provisions. The assessments documented herein cover the design of buildings with PHMF lateral force resisting systems designed according to Chapter 12 of ASCE 7-22 and complying with ACI 550.3 (ACI, 2022). Design coefficients and factors for life-safety design are based on line C.5 of Table 12.2-1 in ASCE 7-22, "Special Reinforced Concrete Moment Frames" (see note *m* of Table 12.2-1 of ASCE 7-22). The response modification factor, R, is 8, overstrength factor, Ω, is 3.0, and the deflection amplification factor, C_d, is 5.5. All designs investigated herein satisfy the life-safety design provisions of ASCE 7-22.

Appendix A of the 2026 NEHRP Provisions provides additional design requirements to satisfy functional recovery performance objectives at the Functional Recovery Earthquake (FRE_R) level shaking. The functional recovery seismic performance factors include the functional recovery response modification coefficient, R_{fr}, functional recovery allowable story drift limit, Δ_{afr}, and the functional recovery structure ductility reduction factor, $R_{\mu fr}$. Drift checks are performed with C_d equal to R_{fr} for functional recovery design.

R_{fr} and Δ_{afr} were determined by developing an archetype space of different building heights, designed with various functional recovery response modification coefficients and allowable drift limits, and then selecting the combination that results in less than a 10% mean probability of Safety-Critical Structural Damage, or P[SCSD], in each performance group, and less than 20% P[SCSD] for any individual archetype, for Functional Recovery Category (FRC) A, B and C. The 10% and 20% thresholds are modified to 15% and 25%, respectively, for FRC D. All analyses are conducted at the Functional Recovery Earthquake (FRE_R) level shaking corresponding to a Seismic Design Category $D_{max,FRE}$ condition with two-point spectral ordinates S_{dsfr} and S_{d1fr} of 1.25g and 0.75g, respectively. The required values of R_{fr} and Δ_{afr} based on analysis are compared to the judgment-based limits according to Appendix A of NEHRP 2026, and the more stringent values are selected. The judgment-based limits of R_{fr} are R/1.5 and R/1.25 for FRC A/B/C and FRC D, respectively. The judgment-based limits of Δ_{afr} are 1.25% and 1.75% for FRC A/B/C and FRC D, respectively. System specific $R_{\mu fr}$ factors are determined by comparing peak floor acceleration demands from the analysis with the seismic floor accelerations from Section A.10.6 in accordance with Section A.8.3.6 procedures in Appendix A of the 2026 NEHRP Provisions.

The proposed R_{fr}, Δ_{afr} and $R_{\mu fr}$ for the PHMF lateral force resisting system from the qualification assessment are presented in Table 1. Results of the evaluation showed that the functional recovery performance factors for PHMFs were primarily governed by damage to the precast primary gravity connections in the mid-rise performance groups, with design criteria governed by the 10% mean acceptance criteria. For PHMFs, a drift limit of Δ_{afr} equal to 1.00% and 1.25% achieves the performance goals for FRC A/B/C and FRC D, respectively, without needing to reduce R_{fr} below the judgment-based limits of R/1.5 = 5.5 and R/1.25 = 6.5, respectively.

For this structural system, the resilient design requirements (drift limits in particular) were controlled by the need to control drift demands on the gravity system. Historically, precast gravity systems have often performed poorly in past earthquakes. Because of this, US design provisions have been updated to provide additional design requirements intended to prevent the damage and failures seen in past earthquakes to precast elements. However, experimental test data are very limited for modern code-compliant gravity system components and connections.

Based on an extensive review of precast gravity systems, including prior performance, available test data, current life-safety code requirements, and industry best practices, several additional requirements for the PHMF system are prescribed to satisfy the functional recovery requirements. The additional requirements for the PHMF system are as follows:

- Diaphragms shall be “Cast-in-place Concrete Equivalent Precast Diaphragms”, as defined in ASCE 7-22 Section 14.2.2.1
- Topping slab thickness shall be greater than or equal to 3 inches
- Diaphragm reinforcement shall be deformed mild steel, and reliance on welded wire mesh to resist diaphragm loads is prohibited
- Steel bearing plates and bearing pads must be used at bearing locations of all gravity system elements, including primary beam to column connections (e.g., at a corbel) and floor element connections (e.g., double tee to primary beam connections). Bearing plates must be embedded in the supported element.

These requirements recommend detailing that is not currently mandated for life-safety but are expected to increase the seismic performance and deformation capacity of precast gravity systems without requiring onerous changes to practice.

In this study, the gravity system fragility functions were developed through literature review, calculations, and judgment to reflect the expected improved seismic performance of the gravity system that modern design protections aim to provide. However, these fragility functions include some conservatism due to the lack of available experimental test data. Experimental testing of precast gravity system element sub-assemblages is recommended. If such test data are created, the fragility functions could be updated to better reflect the deformation capacity of the gravity system. If the tests indicated greater deformation compatibility than assumed in the judgmentally derived fragilities, it is possible that the system parameters could be updated with more relaxed design drift limits. While not expected, if testing indicated lesser deformation compatibility, the design parameters should also be adjusted.

Table 1 - Summary of functional recovery seismic performance factors for PHMF lateral systems complying with ACI 550.3 (ACI, 2022).

	FRC A/B/C			**FRC D**		
	R_{fr}	**Δ_{afr}**	**$R_{\mu f}$†**	**R_{fr}**	**Δ_{afr}**	**$R_{\mu fr}$†**
Analysis results	7.5	1.00%	--	6.5	1.25%	--
Judgment-based upper limit	5.5	1.25%	--	6.5	1.75%	--
Recommendation – PHMF	**5.5**	**1.00%**	**1.40***	**6.5**	**1.25%**	**1.55***

† $R_{\mu fr}$ is only calculated for the recommended seismic performance factors
** Equivalent to the baseline value calculated using R_{fr}*

Contents

1. INTRODUCTION

This report documents the quantification of the functional recovery seismic performance factors for the precast hybrid moment frame (PHMF) system. The assessment is performed in accordance with the proposed Section A.8.3.6 procedures of the 2026 National Earthquake Hazards Reduction Program (NEHRP) Provisions. The functional recovery seismic performance factors include the functional recovery response modification coefficient, R_{fr}, the functional recovery allowable story drift limit, Δ_{afr}, and the functional recovery structure ductility reduction factor, $R_{\mu fr}$. These are the equivalents of the response modification coefficient, R, the allowable story drift limit, Δ_a, and the structure ductility reduction factor, R_μ, used in ASCE/SEI 7 Chapters 12 and 13, but for design for functional recovery.

The PHMF system represents a subset of configurations used to construct precast concrete frames for seismic resistance. Precast frame systems can have emulative or jointed (non-emulative) connections. Emulative connections attempt to replicate the typical stiffness, strength, and energy dissipation of a traditional cast-in-place connection (Kurama et al. 2018). Jointed connections concentrate nonlinear rotations at member ends, typically using unbonded post-tensioning (PT) between members. PT connections allow for large displacement demands at beam-to-column connections through rocking and possess self-centering capabilities, yet cannot provide significant energy dissipation since tendons and members are designed to remain elastic. The term “hybrid connection” refers to the combination of unbonded PT tendons near the member center and mild steel toward the edges. The mild steel contributes to the flexural strength of the connections and provides an energy-dissipation mechanism (through yielding) that combines with the rocking behavior provided by the PT tendons. An illustration of the main components of a precast hybrid connection is shown in Figure 1.

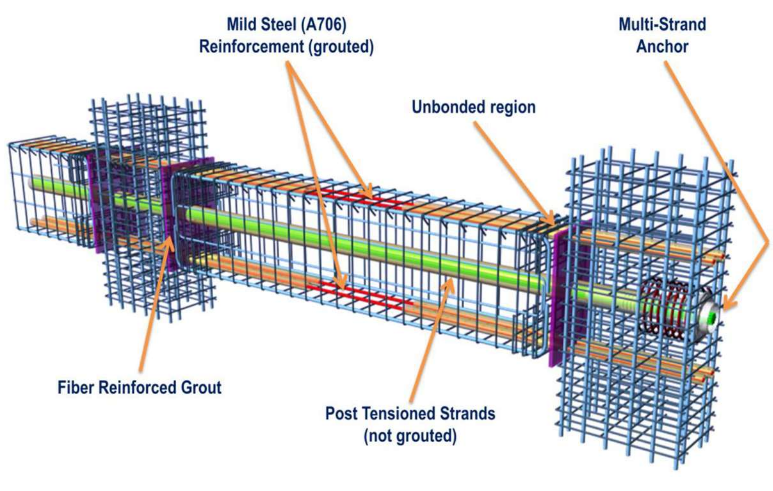

Figure 1. Illustration of the main components of a precast hybrid moment connection. (Image adapted from Clark Pacific, 2015).

The PHMF system is designated as a Special Moment Frame (SMF) according to ACI 318 (ACI, 2019a) and ASCE 7 (ASCE, 2022). All SMFs constructed of precast concrete members must demonstrate equivalency to similar monolithic (cast-in-place) systems by conforming to the requirements of ACI 318 Chapter 18, including testing requirements outlined by ACI 374.1 (ACI, 2019b) to validate connections and the design procedure implemented. The ACI 550.3 (ACI, 2013) design standard was developed specifically for the PHMF system that satisfies ACI 374.1 requirements for connections not explicitly covered by ACI 318 Chapter 18. Systems designed by ACI 550.3 (previously ACI T1.2) are permitted to use the same seismic performance factors (i.e., R, C_d, and Ω_0) as cast-in-place RC SMFs. The PHMF system is required to provide integrity of the entire load path when subjected to a drift demand 3.5% in every story, as defined in ACI 550.3 Section 5.1.2. This capacity is validated through acceptance testing of connections. Additionally, ACI 550.3 Section 5.6 requires that the slab and gravity system components interacting with the lateral system be designed and detailed to accommodate deformations similar to those observed in acceptance testing, such that performance of the diaphragm and the gravity system is not affected. The scope of the current report will pertain to PHMF systems that are compliant with ACI 550.3.

The diaphragm design details are limited to those that can be defined as a “Cast-In-Place Concrete Equivalent Precast Diaphragm,” as defined in ASCE 7-22 Section 14.2.2.1. This class of diaphragm has design loading controlled by ASCE 7-22 Sections 12.10.1 and 12.10.2. Since the introduction of the alternative diaphragm design method in ASCE 7-16 12.10.3, clarifying language has been added by ACI 318-19 and further clarified in ASCE 7-22 with regards to what types of precast diaphragms can still utilize ACSE 7-22 Section 12.10.1 for diaphragm design. A recent article by Ghosh (2022) provides excellent discussion and clarification on the topic.

An archetype space of different building heights, designed with various functional recovery response modification coefficients and allowable drift limits, was developed. FEMA P-58/ATC-138 (FEMA, 2018a; ATC, 2021) models were then created. In accordance with the proposed Section A.8 procedures of the 2026 NEHRP Provisions, only structural components are included in these FEMA P-58/ATC-138 performance models. Design of the archetypes was performed using the automated design capability of SP3 (www.sp3risk.com). Engineering demand parameters (e.g., story drift ratios, peak floor accelerations, etc.) were estimated using SP3’s Response Prediction Engine, where the response is evaluated based on reduced-order elastic models that are adjusted using factors that are statistically calibrated to nonlinear response history analyses of idealized multi-degree-of-freedom models. The SP3 Response Engine does not perform nonlinear response history analyses of the specific archetype directly.

Performance assessments of each model are conducted in accordance with FEMA P-58 (FEMA, 2018a) and ATC-138 recommendations to quantify the probability of safety-critical structural damage (P[SCSD]) for each archetype (Blowes et al., in press). The assigned safety class governs the triggering of SCSD for a given component and damage state according to the ATC-138 methodology. The safety class controls what percentage of components, in each story and direction, that can be in each damage state or greater, prior to triggering SCSD in the building. The P[SCSD] serves as an acceptable proxy for the probability of exceeding the target functional recovery times for structural-only models, as outlined in section CA.8.3.5 of the 2026 NEHRP Seismic Provisions.

The functional recovery seismic performance factors are selected such that archetypes designed for that R_{fr} and Δ_{afr} result in less than a 10% mean P[SCSD] in each performance group and less than 20% P[SCSD] for any individual archetype for Functional Recovery Category (FRC) A, B, and C. The 10% and 20% thresholds are modified to 15% and 25%, respectively, for FRC D. These limits are in accordance with the proposed Section A.8.3.6 procedures of the 2026 NEHRP Provisions. All analyses are conducted at the Functional Recovery Earthquake (FRE_R) level shaking corresponding to a Seismic Design Category $D_{max,FRE}$ condition with two-point spectral ordinates S_{dsfr} and S_{d1fr} of 1.25g and 0.75g, respectively.

2. ANALYSIS METHODS

2.1. Design Iteration and Acceptance Criteria for Seismic Performance Factors

For each individual archetype, design iterations are carried out using values of R_{fr} and Δ_{afr} across the ranges of 1 through R (i.e., up to the response modification coefficient used in life-safety design) and 0.5% through 2.0% (i.e., up to the maximum allowable story drift ratio for Risk Category II structures), respectively. The Response Modification Factor, R, is 8 for PHMF systems, in accordance with Table 12.2-1 of ASCE 7-22 (ASCE, 2022). These design iterations are performed using the SP3 design engine, which estimates the strength and stiffness of each design to determine appropriate structural responses and subsequent estimates of SCSD.

In each performance group, the combination of R_{fr} and Δ_{afr} is deemed to be acceptable if the mean P[SCSD] is less than 10%, and the maximum P[SCSD] across all archetypes in the performance group is less than 20% for quantifying the functional recovery seismic performance factors for Functional Recovery Category (FRC) A, B and C. For FRC D, the mean and maximum P[SCSD] across all archetypes in a performance group must be less than 15% and 25%, respectively. The recommended design values for a particular system are taken as the most restrictive across all performance groups, rounded to the nearest increment considered (0.5 for R_{fr} and 0.25% for Δ_{afr}).

The requirements of the proposed Section A.8.3.6 procedures of the 2026 NEHRP Provisions impose that R_{fr} and Δ_{afr} shall not be taken less than R/1.5 and 1.25% for FRC A, B and C and R/1.25 and 1.75% for FRC D. Additionally, to verify the strength and stiffness coupling inherent to each design variant, each archetype model is re-assessed under an independent strength and stiffness assumption, i.e., where additional strength prescribed by R_{fr} does not result in additional stiffness to the building. Analysis outcomes from the independent-strength-and-stiffness assessment are checked to ensure the maximum P[SCSD] does not exceed the acceptance criteria (20% for FRC A/B/C and 25% for FRC D), where applicable. The judgment-based upper limit and the independent-strength-and-stiffness check provide a reasonable limit, preventing excessive reliance on the analytical results and recognizing the historical precedent set by the higher Risk Categories.

2.1.1. Safety-Critical Structural Damage (SCSD)

The assigned safety class governs the triggering of SCSD for a given component and damage state according to the ATC-138 methodology (ATC, 2021). The safety class controls the percentage of components in each story and direction that can be in each damage state or greater before triggering SCSD. A summary of the ATC-138 safety class descriptions and acceptance thresholds is shown in Table 2.

Table 2. ATC-138 safety-class definitions for triggering SCSD (ATC, 2021).

Safety Class	Description	Acceptance Threshold[a]
0	Slight damage that is not a safety concern and will never trigger an unsafe placard	N/A
1	Moderate damage that may be visually concerning, but does not substantially reduce the lateral strength of the component.	50%
2	Severe damage that causes substantial loss of lateral strength of the component, but does not substantially reduce its vertical load-carrying capacity.	25%
3	Severe damage that compromises both the lateral and vertical load-carrying capacity of the component.	10%

[a] Percentages reflect the upper quantity of components, in each story and direction, that can be in a safety class of interest before triggering safety-critical structural damage (SCSD). The safety critical structural damage check is performed independently for each independent system in the building (e.g., the gravity vs. lateral system).

2.2. Fragility Functions for Precast Hybrid Moment Frame Systems

Fragility functions relate structural responses to the likelihood of damage and its consequences. Fragility functions are commonly modeled by a lognormal distribution defined by a lognormal mean (θ) and standard deviation (β). For a given structural component, sequential damage states (DSs) can be represented by individual fragility functions that describe the likelihood of a distinct level of damage, the corresponding level of repair effort, and the associated consequences. Additionally, damage states may be mutually exclusive, with a single fragility function representing multiple outcomes (i.e., sub-damage states). Each likelihood is assigned a weighting that sums to unity (e.g., 0.25 + 0.75 = 1). The fragility functions used in the current study will use both sequential and mutually exclusive damage state definitions. More general background information on fragility functions and damage state development can be found in FEMA P-58-1 (FEMA, 2018a).The following sub-sections provide details on the structural component fragility functions, including:

- PHMF beam-to-column connections
- Precast gravity connections

Foundation elements are considered rugged in the current analysis. Fragility functions for foundation elements were not developed during the FEMA P-58 project, and foundation elements are specifically included in the list of acceptable rugged components in Appendix I of FEMA P-58-1 (FEMA, 2018a).

2.2.1. Precast Hybrid Moment Frame Beam-to-Column Connection Fragilities

PHMF beam-to-column connection fragilities were developed within a previous study conducted for Clark Pacific (Fitzgerald et al. 2016). The fragility development is based on experimental testing of hybrid beam-to-column connection sub-assemblies (Stanton et al. 1997; Kim et al. 2004; Pastrav and Enyedi, 2012) and multiple connections on a scaled 5-story full frame test (Priestley et al. 1999). A total of 14 beam-to-column connections were used for fragility development. The connections include planar beam-columns with beams on both sides, one side, and exterior corner assemblies. A summary of the experimental studies is provided in Table 3.

Table 3. Experimental testing used for hybrid beam-to-column connection fragility development (Fitzgerald et al. 2016)

References	Assembly Type	Loading Protocol
Kim et al. (2004)	Plane beam-column (BC) segment with a beam on each side	Column pinned at top and bottom and beam end(s) cycled in opposition at amplitudes increasing by 25% every 3 cycles.
	Plane BC segment with a beam on one side	
	Corner element	Column pinned at top and bottom, and beam ends cycled in opposition at amplitudes increasing every 3 cycles; additionally, beams were displaced in the same direction together at specific drifts.
	Corner element	
Stanton et al. (1997) [a]	M-P-Z4	Beam ends restrained with roller connections, column pinned at base, column top cycled at increasing amplitudes every 3 cycles separated by an elastic cycle.
	N-P-Z4	
	O-P-Z4	
	P-P-Z4	
Priestley et al. (1999)	1st story 1/3 scale frame	Pseudo-dynamic testing using earthquake segments defined at multiples (0.33, 0.50, 1.0, 1.5) of a design level earthquake.
	2nd story 1/3 scale frame	
	3rd story 1/3 scale frame	
Pastrav and Enyedi (2012)	Plane BC segment with a beam on each side	Beam ends restrained with roller connections, column pinned at base, column top cycled at increasing amplitudes every 3 cycles separated by an elastic cycle.

[a] All test specimens are a plane beam-column (BC) segment with beams on both sides

Fragility functions for PHMF beam-to-column connections were developed following FEMA P-58-1 Appendix H (FEMA, 2018a). The fragility functions are comprised of three sequential damage states (DS), using peak interstory drift ratio as the engineering demand parameter. DS1 represents concrete spalling and the onset of visible damage requiring repair. DS2 represents the fracture of the mild steel continuity bars and is associated with a significant (20%-25%) drop in strength of the beam-column assembly. DS3 represents yielding of the post-tensioning (PT) tendons. A summary of the PHMF beam-to-column connection fragility functions, and corresponding safety classes, is provided in Table 4. An illustration of the three damage states of PHMF connections is provided in Figure 2. A plot of the fragility functions is provided in Figure 3. Additional details of PHMF connection fragility development can be found in Fitzgerald et al. (2016).

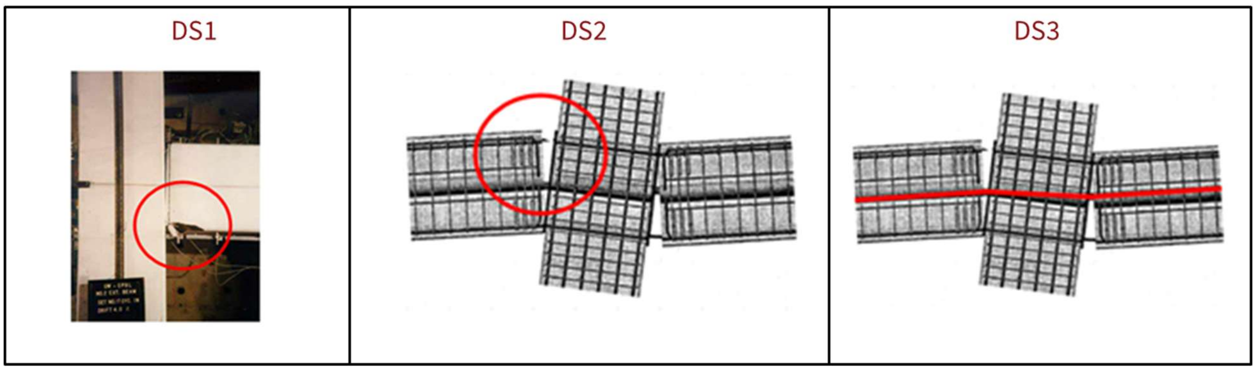

Figure 2 – Illustration of damage states for precast hybrid moment connections (Fitzgerald et al. 2016).

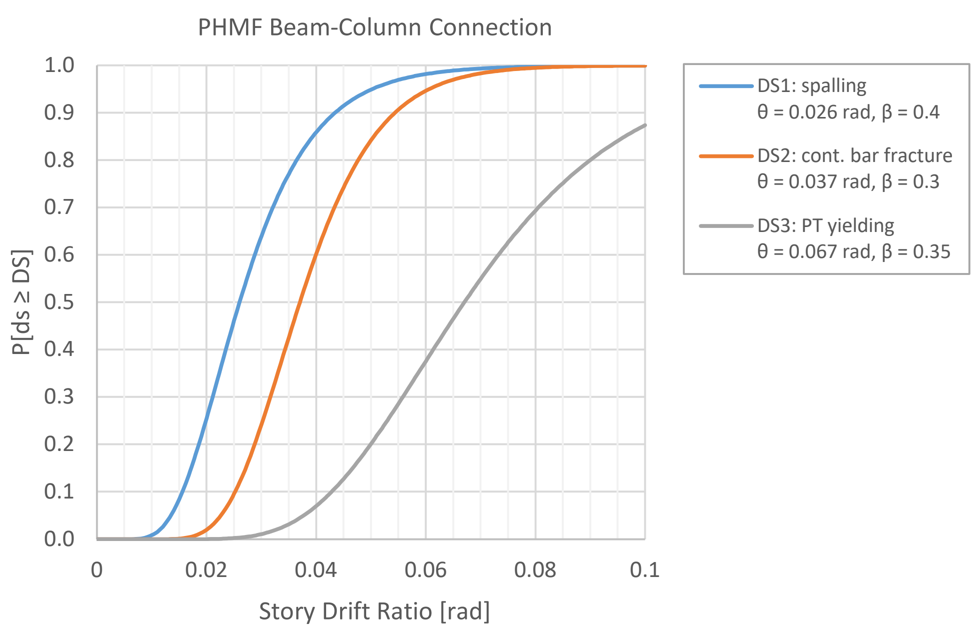

Figure 3 – Fragility functions for precast hybrid moment connections. Damage state details are provided in Table 4.

Table 4 – Precast hybrid moment frame beam-to-column connection fragility damage states and corresponding safety classes.

Damage State	Median (θ)[a]	β	Safety Class[b]	Damage Description	Repair Measures
DS1	2.6%	0.40	0	*Concrete Spalling*: Beams or possibly joints exhibit spalling of cover concrete.	Remove furnishings, ceilings, and mechanical, electrical, and plumbing systems (as necessary) 8 feet on either side of the damaged area. Clean the area adjacent to the damaged concrete. Prepare spalled concrete and adjacent cracks, as necessary, to be patched and to receive the epoxy injection. Patch concrete with grout. Replace and repair finishes. Replace furnishings, ceilings, and mechanical, electrical, and plumbing systems as necessary.
DS2	3.7%	0.30	2	*Continuity Bars Fracture*: One or more mild steel continuity bars fracture in or near the region of the beam column interface such that the strength of the beam column element is decreased by 20%-25%.	Remove furnishings, ceilings, and mechanical, electrical, and plumbing systems (as necessary) 8 feet on either side of the damaged area. Provide shoring and remove concrete necessary to access ruptured mild steel. Remove the mild steel, leaving the core of the beam and the grout pad intact (this allows the PT stress to be maintained through the repair process). Core through the joint to remove the mild steel that passes through the joint. Replace mild steel through the joint and provide mechanical coupling to the remaining bar anchored in beam. Pour concrete to replace the mass spalled and chipped out. Replace and repair finishes. Replace furnishings, ceilings, and mechanical, electrical, and plumbing systems as necessary.
DS3	6.7%	0.35	2	*Post Tension Cable Yields*: The PT strand running through the beam-column section yields. This damage state will affect all similar fragilities between the PT tendon anchors.	Remove end caps and determine the level of damage to the PT strand. Remove furnishings, ceilings, and mechanical, electrical, and plumbing systems (as necessary) 8 feet on either side of the damaged area. Clean area adjacent to the damaged concrete. Provide shoring and remove concrete necessary to access ruptured mild steel. Remove the mild steel, leaving the core of the beam and the grout pad intact. Core through the joint to remove the mild steel that passes through the joint. Replace mild steel through the joint and provide mechanical coupling to remaining bar anchored in beam. Pour concrete to replace the mass spalled and chipped out. Replace and repair finishes. Replace furnishings, ceilings, and mechanical, electrical, and plumbing systems as necessary. If necessary, replace the PT strand; else, re-tension the PT strand to obtain the desired stress level.

[a] Fragility function is a lognormal distribution with median and standard deviation of θ and β, respectively. The EDP is story drift ratio.

[b] SC 1 = 50%, SC 2 = 25%, SC 3 = 10% allowable quantity of damaged component per direction per story; SC 0 cannot cause SCSD.

2.2.2. Precast Gravity Connection Fragilities

Precast gravity connection fragilities are based on a study conducted by HB-Risk for Clark Pacific. Due to a lack of experimental test data for modern precast gravity assemblies, the fragilities presented herein are based on engineering judgement informed by an extensive review of the treatment of modern gravity connections in precast construction, as well as review of precast gravity system behavior following recent seismic events. This is followed by the definition of damage states, selection of engineering demand parameters, and the final fragility function summary.

Code Considerations for Precast Concrete Gravity Systems

Design provisions within ACI 318-19 (ACI, 2019) for precast gravity systems are largely governed by Section 16.2 (Connections of precast members) and Section 18.14 (Members not designated as part of the seismic-force resisting system) for structures in Seismic Design Category (SDC) D, E, and F.

Section 16.2 of ACI 318-19 has three critical requirements for all precast concrete connections:

- 16.2.1.2 – Adequacy of connections shall be verified by analysis or test.
- 16.2.1.3 – Connection details that rely solely on friction caused by gravity loads shall not be permitted.
- 16.2.1.4 – Connections, and regions of members adjacent to connections, shall be designed to resist forces and accommodate deformations due to all load effects in the precast structural system.

ACI 318-19 Section 18.14.4.1 (precast beams and columns) has the following requirements for gravity system members:

a) Requirements of 18.14.3 (requirements for cast-in-place gravity members).
b) Ties specified in 18.14.3.2(b) over the entire column height, including the depth of the beams.
c) Structural integrity reinforcement, in accordance with 4.10.
d) Bearing length at the support of a beam shall be at least 2 in. longer than determined from 16.2.6.

Commentary for Section 18.14.4.1 has been largely unchanged since ACI 318-02 and reads as follows:

"Damage to some buildings with precast concrete gravity systems during the 1994 Northridge earthquake was attributed to several factors addressed in this section. Columns should contain ties over their entire height, frame members not proportioned to resist earthquake forces should be tied together, and longer bearing lengths should be used to maintain integrity of the gravity system during ground motion. The 2 in. increase in bearing length is based on an assumed 4 percent story drift ratio and 50 in. beam depth, and is considered to be conservative for the ground motions expected for structures assigned to SDC D, E, or F. In addition to this provision,

precast frame members assumed not to contribute to lateral resistance should also satisfy the requirements for cast-in-place construction addressed in 18.14.3, as applicable (ACI 318-19 R18.14.4.1)".

Examples of precast gravity system failures observed from the 1994 Northridge earthquake, the mitigation of which is in line with the intent of ACI 318-19 Section 18.14, are provided in Figure 4. The increase in bearing length required by ACI 318-19 18.14.4.1d) is illustrated in Figure 5. Similar to the commentary of ACI 318-19 16.2.6, Figure 5 differentiates between the bearing length ($L_{bearing}$) and length of the end of a precast member over support ($L_{end\text{-}to\text{-}support}$). Lower Seismic Design Categories (i.e., SDC C and lower) are required to provide $L_{end\text{-}to\text{-}support}$ in accordance with ACI 318-19 16.2.6, where SDC D, E, and F must provide $L_{bearing}$ in accordance with 16.2.6, plus an additional 2 inches. This is an important distinction since it reflects a considerable increase in bearing length for higher SDC structures. The mention of the target drift capacity of 4% assuming a 50-inch beam depth in ACI 318-19 18.14.4.1 commentary (see above) can only be related to the simple kinematic relationship that 2 in./ 50 in. results in 0.04 radians of rotation. All accessible versions of ACI 318 were reviewed and no further discussion or justification is provided. Importantly, the additional 2 inches of bearing length is not a function of beam depth, so a beam with a depth of 24 inches would be provided with 0.083 radians of protection against unseating.

Figure 4 – Examples of poor design detailing that led to failure of precast gravity systems during the 1994 Northridge earthquake: a) failure of interior gravity column (fib, 2003); b) failure of exterior gravity column (Todd et al. 1994); c) unseating of double tee beam (Iverson and Hawkins, 1994); d) unseating of hollow core floor section (fib, 2003).

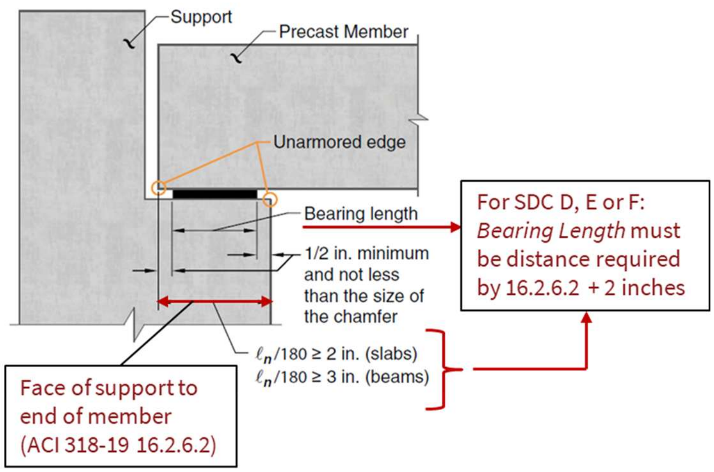

Figure 5 – Illustration of increased bearing length required for beams in SDC D, E, and F compared to face to end dimensions required for low seismic design categories (Figure adapted from Figure R16.2.6 of ACI 318-19)

Section 12.12.4 of ASCE 7-22 states:

"For structures assigned to SDC D, E or F, every structural component not included in the seismic force-resisting system in the direction under consideration shall be designed to be adequate for the gravity load effects and the seismic forces resulting from the Design Earthquake Displacement (δ_{DE}) and the associated drifts as determined in accordance with Section 12.8.6."

The only exception to ASCE 7-22 §12.12.4 is that reinforced concrete frame members not designated as part of the seismic force-resisting system shall comply with Section 18.14 of ACI 318, which was previously discussed. The commentary for ASCE 7-22 §12.12.4 uses failure of precast gravity systems from the Northridge event (see Figure 4 for examples) as an example and states the following about the exception to §12.12.4:

"The exception is intended to encourage the use of intermediate or special detailing in beams and columns that are not part of the seismic force-resisting system. In return for better detailing, such beams and columns are permitted to be designed to resist moments and shears from unamplified deflections. This design approach reflects observations and experimental evidence that well-detailed structural components can accommodate large drifts by responding inelastically without losing significant vertical load-carrying capacity,"

Notably, no supporting references are provided in the commentary for the exception to ASCE 7-22 §12.12.4, yet this exception further emphasizes the expected performance of concrete gravity systems in compliance with ACI 318 §18.14.

This discussion of the code considerations for precast gravity systems is important to both inform the reader of the numerous considerations required for this type of structural system as well as the general code expectation of conforming design in terms of life safety performance. As highlighted, precast gravity systems conforming to ACI 318-19 are expected to achieve the basic life safety goals of the code, or conversely, prevent adverse structural response that would jeopardize such goals.

Development of Damage States

Damage states for precast gravity systems were developed through review of damage documentation in recent New Zealand seismic events, including the 2010 (Darfield/Canterbury) and 2011 (Lyttleton) Christchurch sequence, and the 2016 Kaikoura earthquake (Kam et al. 2010; Kam et al. 2011; Corney et al. 2014; Henry et al. 2017). New Zealand events were utilized as opposed to the 1994 Northridge event, since more documentation is available for damage behavior of precast framing. Damage states target "pre-collapse" conditions of the gravity system, and assume that complete unseating of framing elements is considered a structural collapse (whether partial or total). This is consistent with the treatment of flat plate slab connection fragilities within FEMA P-58 (Gogus and Wallace, 2008) that include the onset of punching failure as a final damage state, but do not attempt to represent complete loss of vertical load carrying capability with a modeled damage state.

The damage state (DS) structure assumes two sequential DS, referred to as DS1 and DS2, respectively. DS2 is split into two mutually exclusive damage states (i.e., DS2a and DS2b). Damage State 1 (DS1) considers similar damage expected for the DS1 of Precast Hybrid Moment frame connections (see Table 4), including cracking of the topping slab and the possibility of minor spalling in flooring or primary beam elements. Some illustrations of DS1 are provided in Figure 6.

a) b) c)

Figure 6 – Examples of damage attributed to damage state 1: a) cracking of topping parallel to beam (Henry et al. 2017); b) cracking of slab between floor unit joints (Corney et al. 2014); c) minor spalling of primary beam (Henry et al. 2017)

The definition of Damage State 2a and 2b considers the different severities of member and connection damage. Henry et al. (2017) used a Critical Damage State (CDS) hierarchy to document observed damage to precast floor systems following the 2016 Kaikoura earthquake. CDS A and B represent damage that could lead to compromised gravity load path under gravity loads only (CDS A) and considering the possibility of additional lateral (aftershock) loading (CDS B). CDS C represents damage that is commonly observed following significant seismic loading but does not pose additional risk of structural collapse. DS2a is aimed at capturing CDS

C level damage, while DS2b targets damage that would minimally be associated with CDS B or worse. DS2a considers significant spalling and cracking of floor (deck) and primary members, yet assumes that the damage is not critical for maintaining vertical load carrying capacity. Some example illustrations of DS2a are provided in Figure 7.

a) b) c)

Figure 7 – Examples of damage attributed to damage state 2a: a) spalling of primary beam at dapped double tee connection (Corney et al. 2014); b) cracking and spalling of double tee flange (Corney et al. 2014); c) spalling of primary beam from hollow core section above (Kam et al. 2010)

DS2b considers cracking and connection damage that is likely to render the remaining gravity load carrying capacity of the gravity system questionable. Examples of DS2b damage are provided in Figure 8. The cracking pattern in Figure 8b shows a vertical crack forming vertically in the web of a double tee beam, extending vertically from the dapped support. Depending on the severity of the cracking, the element shown in Figure 8b could be approaching a direct shear failure condition (PCI, 1988). This is contrary to the cracking shown in Figure 7b, where cracking and spalling limited to the flange of a double tee could be less of a concern since the development of a failure mechanism in the member is not apparently imminent and flange cracking in double tees is typically not a concern for remaining gravity load carrying capacity (Henry et al. 2017).

a) b) c)

Figure 8 – Examples of damage attributed to damage state 2b: a) hollow core section cracking through thickness near support (Kam et al. 2010); b) vertical cracking of double tee web at dapped connection (Corney et al. 2014); c) connection damage of flange-hung double tee with vertical settlement indicating unseating is possible (Kam et al. 2011)

The damage depicted in Figure 8c represents an extreme case of flange-hung double tees failing at the bearing connection with visible vertical displacements, indicating that unseating of the connection may be imminent upon further loading. Notably, the detailing used in in Figure 8c is known as a “pig tail” or “loop bar” connection that was a very common detail for double tee connections in New Zealand. These connections have been shown to be non-compliant with the intent of the building code (Hare et al. 2009) and have since been disallowed (Corney et al. 2014; Hare et al. 2018; MBIE, 2018).

Judgment-based Fragility Parameters

The fragility parameters used to represent the behavior of precast gravity system components are discussed in this section. Fragility functions are developed for primary gravity beams and double tee assemblies.

The engineering demand parameter (EDP) selected is story drift ratio. The use of story drift ratio was deemed the clearest for developing the fragilities based on judgment. The actual demands that can cause various types of damage to precast gravity components are likely a mix of principal direction story drift demand, torsional displacement demand, as well as vertical and horizontal force (i.e., acceleration) demands. This assumption to simplify the treatment of EDPs is made to maintain a level of simplicity that is suitable for FEMA P-58 assessment and inherently assumes that other EDPs not directly considered are reasonably represented by story drift demand.

The median story drift corresponding to DS1, the onset of cracking in the topping slab, was judged to occur at a similar level of demand as DS1 for the PHMF connections (see Table 4), with a median value of 2.5% drift and a dispersion of 0.3. DS1 is assigned a safety class of zero and therefore, has no impact on the performance outcomes for safety-critical structural damage. The attribution of Safety Class 0 to DS1 was supported by the additional requirements of an increased minimum topping thickness of 3 inches and not allowing welded wire mesh reinforcement to transfer diaphragm shear.

The median story drift ratio associated with DS2 (i.e., DS2a and DS2b) was initially based on the typical gap sizes provided between precast members to allow for volumetric changes (i.e., due to creep, shrinkage, and temperature). Typical details for connections of the primary gravity beams into both frame and gravity columns are shown in Figure 9. Typical details for double tee connections (using flange hangers) are shown in Figure 10. The primary beam details in Figure 9 show that a 1.25-inch gap is specified between beams and columns. The flange-hung double tee details in Figure 10 show that a 0.75-inch gap is specified at the top of the double tee near the hanger. The change in dimension of the double tee along the depth represents the draft angle that is common for manufacturing hung double tees and is commonly 0.75 to 1.0 inch over the depth of the member (Roskelley, 2025). This would provide a gap of 1.5 to 1.75 inches between the bottom of the double tee and the primary beam (see Figure 9a). Notably, double tees with dapped ends (i.e., bearing on an inverted T-beam) typically have separation gaps similar to primary beam members (Ghosh et al. 2017).

(a) (b)

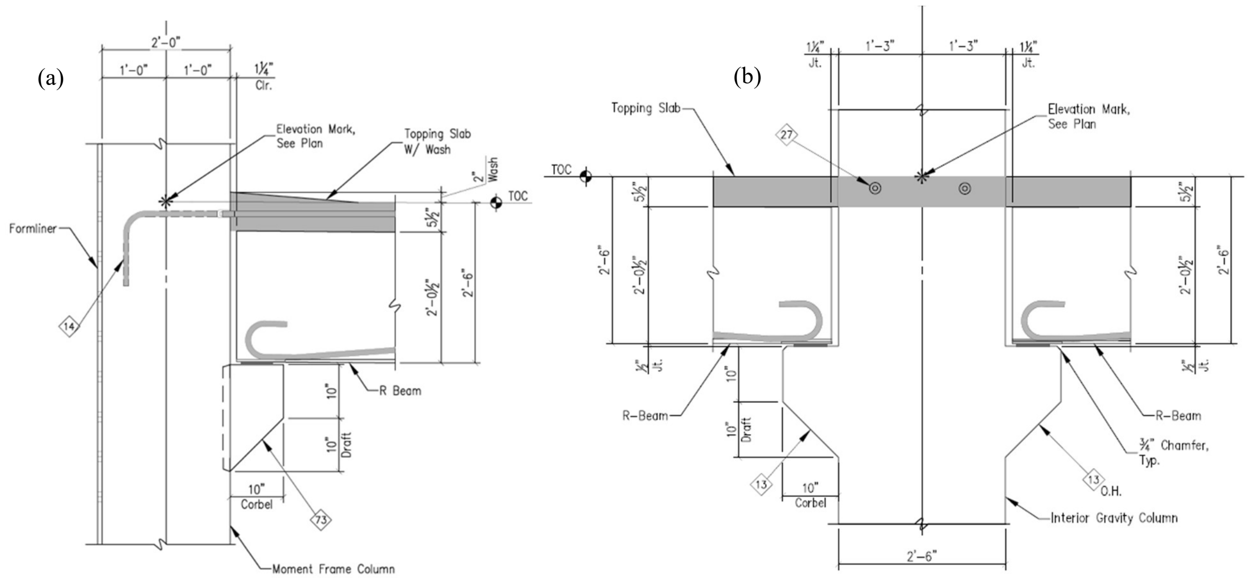

Figure 9 – Standard Precast Primary Gravity Beam Connections for both (a) exterior and (b) interior configurations (courtesy of Clark Pacific).

The typical gaps provided for volumetric change and construction produced drift ratios in the range of 3.0% to 5.0%, depending on the effective beam depth (e.g., 24 to 50 inches). This was eventually deemed too permissive for the shallower beam depths, due to lack of experimental evidence and considerations of erection tolerances on the available gap between precast elements. The final assumption for the treatment of DS2 was to assume a median capacity of 3.5%, that is the required lateral system capacity according to ACI 550.3. A dispersion of 0.25 was applied to this median to account for uncertainty in erection tolerances, member depths, detailing, and the judgemental basis for the fragility development.

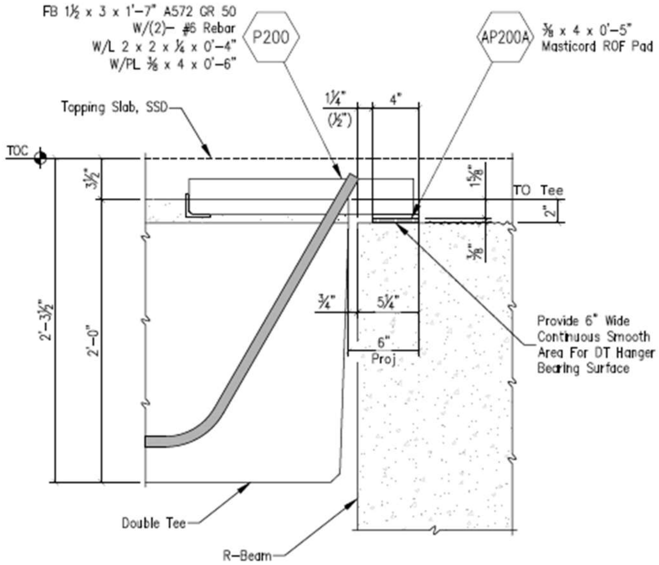

a)

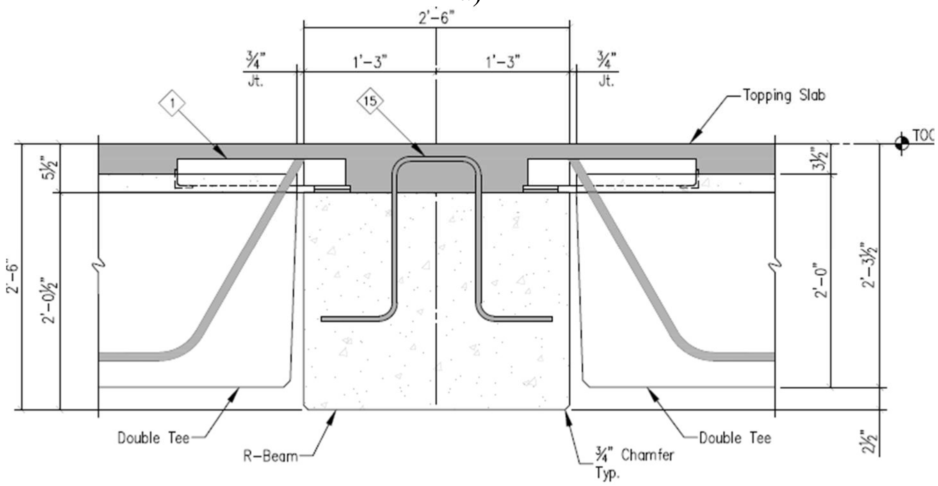

b)

Figure 10 – Standard flange-hung double tee to primary beam connections for both (a) exterior and (b) interior configurations (courtesy of Clark Pacific).

For the precast concrete primary gravity beam connection, damage initially accumulates in the form of cracks and spalling in the topping slab and minor spalling in the precast elements; as drift increases, more significant damage may begin to accumulate in the beam, column, and corbel. As story drift reaches 3.5% and beyond, cracking and spalling will become more serious, possibly extending into the beam, column, and corbel. At this upper damage state, there may be bearing offset and reduced connection capacity, either through loss of bearing length or damage to precast elements. The progression of damage in the precast gravity connections, for both the primary beam and double tee connections, is binned into two distinct damage states, as outlined in Table 5. The second damage state consists of two mutually exclusive damage states. The 50% weighting assigned to DS2a and DS2b reflects the judgmental basis for these fragilities, without explicit experimental data for verification.

Table 5 – Precast concrete gravity connection fragility damage states and corresponding safety classes. Applies to both the primary gravity beam connections and the double tee beam connections.

Damage State	Median (θ)[a]	β	Safety Class[b]	Damage Description	Repair Measures
DS1	2.5%	0.30	0	*Residual cracks in the slab and minor spalling in precast elements.*	Epoxy injection of cracks and grout spalled concrete.
DS2a (50%)	3.5%	0.25	1	*Significant Slab Cracking & Spalling.* Yielding of reinforcement, column, beam, or corbel damage may be visually concerning.	Repair spalled concrete and adjacent cracks, as necessary, to be patched and to receive the epoxy injection. Patch concrete with grout
DS2b (50%)	3.5%	0.25	3	*Bearing offset.* Significant spalling in the topping slab, exposing the connection reinforcement. Visible damage to the beam, column, and corbel, with bearing offset and reduced bearing length possible. The remaining integrity of the connection is questionable.	Repair the damaged connection. Repair beam, column, and corbel damage, as applicable. Shoring and re-centering may be required.

[a] Fragility function is a lognormal distribution with median and standard deviation of θ and β, respectively. The EDP is story drift ratio.
[b] SC 1 = 50%, SC 2 = 25%, SC 3 = 10% allowable quantity of damaged component per direction per story; SC 0 cannot cause SCSD.

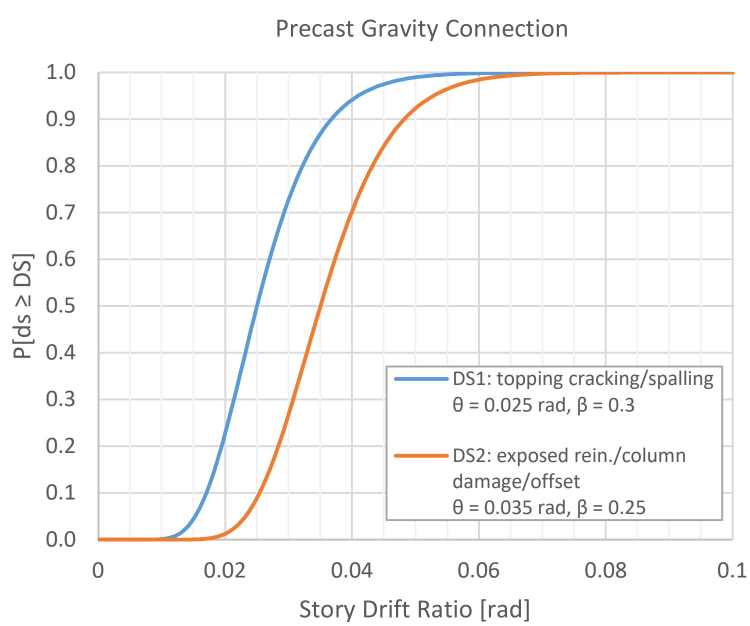

Figure 11 - Fragility functions for precast gravity connections. Damage state details are provided in Table 5.

2.3. Archetypes Considered for Analysis

To determine the combination of R_{fr} and Δ_{afr} that results in acceptable functional recovery performance, an archetype space is divided into performance groups, analyzed, and the overall parameters are determined by the worst-case performance group. This is similar to the FEMA P-695 methodology used for quantifying performance factors for life-safety (FEMA, 2009) and is in accordance with the proposed Section A.8 procedures of the 2026 NEHRP Provisions.

The PHMF system has an archetype space comprising three performance groups and a total of 12 individual archetype variants. The background on the development of the archetype design space is presented in the following sub-sections.

2.3.1. Building Configuration and Structural Component Population

All archetypes assume a constant plan area of 100 feet by 100 feet. Story heights are assumed to be 15 and 13 feet for the first and typical stories, respectively.

The PHMF archetypes assume a bay spacing of 25 feet in each principal direction. The moment frames are assumed to extend along the entire perimeter of the building, comprising four bays on each side. In the performance model, four interior precast moment frame connections (i.e., frame beam connections on both sides of the column) are populated on each side of the building on each story (eight per direction, 16 per story), which ensured an equivalent number of frame beams and columns per the design of the lateral force-resisting system (LFRS). An illustration of the plan layout and populated moment connection assemblies for the PHMF archetypes is provided in Figure 12.

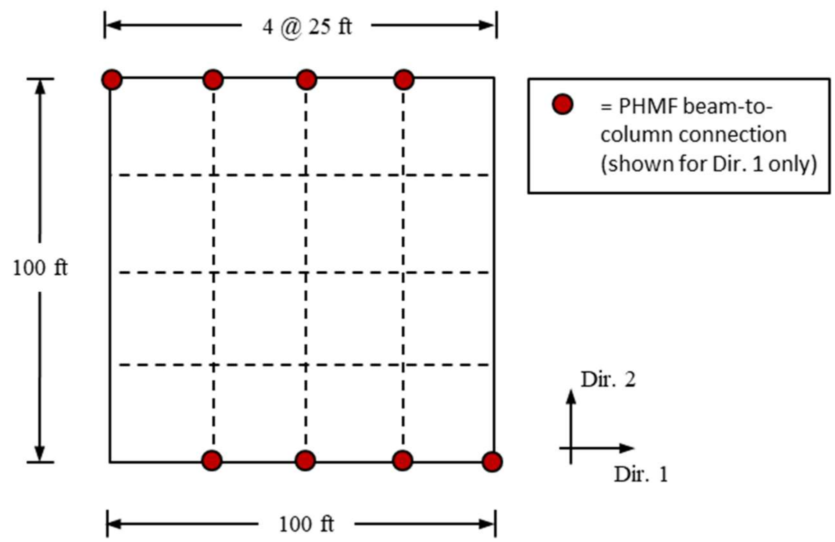

Figure 12. Illustration of the assumed plan layout and structural component population of the PHMF connections. Moment connection assemblies are only shown for Direction 1.

Gravity systems assume a primary one-way beam and column line in one direction and double tees in the other direction. Primary gravity system beam-to-column connections (i.e., at corbels) are populated as interior (beams on both sides) and exterior (beam on one side) assemblies.

Similarly, double tee connections populate interior (tees on both sides of the primary beam) and exterior locations. An illustration of the plan layout and populated gravity system components for the PHMF archetypes is provided in Figure 13.

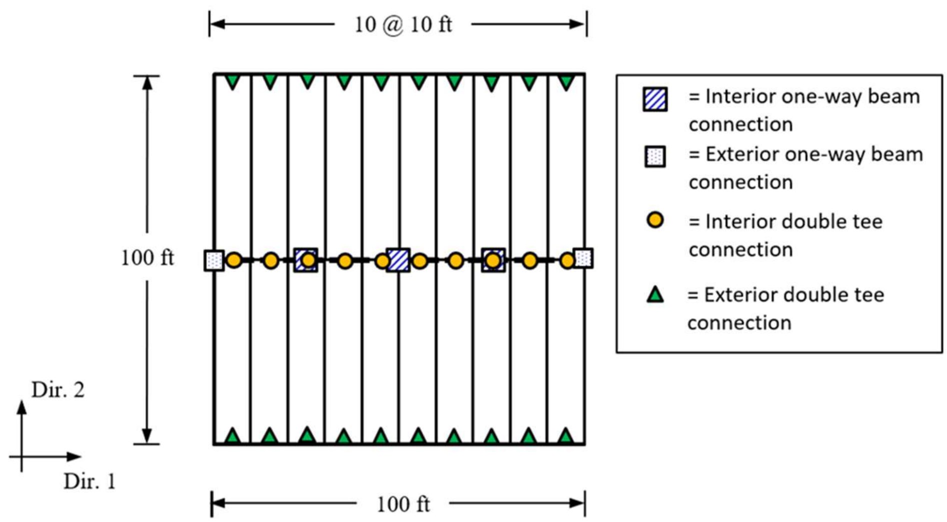

Figure 13. Illustration of the assumed plan layout and structural component population of the precast gravity system. Double tees are spaced at 10 feet on center. Rugged gravity system archetypes do not populate these components.

2.3.2. Performance Groups for PHMF

The performance groups considered for the PHMF system were low-, mid-, and high-rise buildings of the heights used in determining seismic performance factors for life-safety using FEMA P-695 analysis for RC special moment frames (Haselton and Deierlein, 2007; FEMA, 2009; Haselton et al., 2011b). The building height ranges (i.e., number of stories) in each performance group are shown in Table 6.

Table 6. Summary of precast hybrid moment frame performance groups.

Performance Group	Stories
PG1	1, 2, 3, 4
PG2	6, 8, 10, 12
PG3	14, 16, 18, 20

2.4. Estimation of Structural Responses

The structural responses for the archetypes were determined using the SP3 Structural Response Prediction Engine (SRPE) (Cook et al. 2018). The SRPE generates a simplified linear multi-degree-of-freedom model representative of strength and stiffness requirements. Nonlinear response is determined by modal analysis, which is then modified to account for the nonlinear behavior of the system. The expected nonlinear behavior is calibrated by sampling from Incremental Dynamic Analysis (IDA: Vamvatsikos and Cornell, 2002) results from high-fidelity nonlinear models of moment frame buildings.

The following sections provide an overview of the analytical basis behind the SRPE and the quantification of different Engineering Demand Parameters (EDPs). This section focuses on the prediction of median response conditioned on spectral acceleration (Sa). Record-to-record uncertainty and modeling uncertainty are modeled according to FEMA P-58 (FEMA, 2018b).

2.4.1. Analytical Basis Behind the Moment Frame SRPE in SP3

The SRPE moment-resisting frame submodule is used to estimate structural responses for PHMF systems in this assessment. The SRPE sub-module for moment-resisting frames was developed with a large inventory of nonlinear response-history analyses of both reinforced concrete and steel moment frames, including concrete frames with both ductile and non-ductile detailing. In calibrating the SRPE responses for moment frame systems, it was found that both steel and concrete frames have relatively similar responses and nonlinear response localization. However, differences arise in periods and mode shapes, the strong-column weak-beam design, and the level of element ductility capacity. The PHMF system is expected to behave similarly to the RC Special Moment Frame system because PHMF connections are required to have equivalent ductility to similar monolithic (cast-in-place) components, and because similar strong-column, weak-beam requirements are enforced.

The RC Moment Frame SRPE is calibrated to a subset of 30 ductile (Haselton and Deierlein, 2007; Haselton et al., 2011b) and 26 non-ductile (Liel and Deierlein, 2008; Liel et al., 2011) building archetypes. Buildings were modeled in 2D using OpenSees (McKenna et al. 2010) using nonlinear elements calibrated to experimental databases (Haselton et al. 2016). These models were previously used in the initial development of the FEMA P-695 (FEMA, 2009) methodology for quantifying performance factors for life-safety (Liel et al., 2009; Haselton et al., 2011a). Additionally, several ordinary moment frame (OMF) models were used for calibration for buildings in areas of lower seismicity.

A summary of the different archetype buildings considered for SRPE calibration for RC special moment frames is provided in Table 7. The models consist of building heights ranging from 1 to 20 stories. Both perimeter and space frame configurations are considered. Additional variations include the bay length, base fixity, and the presence of weaker lower stories. All models were analyzed using the FEMA P-695 far-field ground motion set (FEMA, 2009), consisting of 44 ground motions (i.e., 22 horizontal pairs). Incremental Dynamic Analysis (IDA: Vamvatsikos and Cornell, 2002) was used to obtain a range of linear and nonlinear structural responses for calibration. The key EDP for structural response prediction of the PHMF system is peak story drift ratio for the estimation of SCSD. An overview of the estimation of this EDP is discussed in the following sub-section.

Table 7. Summary of building models used for calibration of the RC Special Moment Frame SRPE. Table adapted from Haselton et al. (2011b).

ID	No. Stories	Framing	Design Case	ID (cont'd)	No. Stories	Framing	Design Case
2061	1	Space	Baseline[a]	1022	8	Space	Uniform
2062	1	Space	Pinned	2065	8	Space	WS-1 (65%)[d]
2063	1	Space	Fixed	2066	8	Space	WS-1 (80%)
2069	1	Perimeter	Baseline	1023	8	Space	WS-2 (80%)
1001	2	Space	Baseline	1024	8	Space	WS-2 (65%)
1001a	2	Space	Pinned	1013	12	Perimeter	Baseline
1002	2	Space	Fixed	1014	12	Space	Baseline
2064	2	Perimeter	Baseline	1015	12	Space	Uniform
1003	4	Perimeter	Baseline	2067	12	Space	WS-1 (65%)
1004	4	Perimeter	Uniform[b]	2068	12	Space	WS-1 (80%)
1008	4	Space	Baseline	1017	12	Space	WS-2 (80%)
1009	4	Perimeter	L_{bay} = 30 ft[c]	1018	12	Space	WS-2 (65%)
1010	4	Space	L_{bay} = 30 ft	1019	12	Space	L_{bay} = 30 ft
1011	8	Perimeter	Baseline	1020	20	Perimeter	Baseline
1012	8	Space	Baseline	1021	20	Space	Baseline

[a] Baseline design case considers rotational stiffness of grade beams and any basement stories. Pinned and fixed alternatives adjust what is assumed in design.

[b] Conservative design with constant member sizes and reinforcement over building height

[c] Baseline designs have 20 ft bay spacing, alternates have 30 ft bay spacing

[d] WS-1 is for designs with only the first story being weak, and WS-2 is for the 1st and 2nd stories being weak. Percentage is that of strength between the weakened stories and the story above.

2.4.2. Structural Properties Estimation

Building structural properties are estimated using a linear building model, with strength and stiffness scaled to meet corresponding design requirements. Typical levels of overstrength (e.g., due to expected material properties, etc.) are added after design requirements are satisfied, to provide the best possible estimate of the true strength and stiffness of the LFRS. The commercial version of SP3 also includes additional strength and stiffness contributions from the gravity system and nonstructural components, but these are excluded in this study for compliance with the procedures of Section A.8 of the 2026 NEHRP Provisions.

The process begins by determining the design parameters, including spectral values, response modification factor (R), deflection amplification factor (C_d), and related values (e.g., I_e). Next, a target seismic design drift is selected. For drift-controlled systems, such as most moment frames, this target is typically the design drift limit—for example, 2% for risk category II buildings. For strength-controlled systems, the target drift is a realistic value appropriate for the system type and building height; the expected design drift values are based on a database of hundreds of building designs (from archetype buildings in the SP3 SRPE database). Resilient design iterations use the same process with pairs of R_{fr} and Δ_{afr} for a given analysis. Notably, the deflection amplification factor for functional recovery (C_{dfr}) is taken equal to R_{fr}, and the building importance factor (I_e) is taken as unity per Section A.8 of the 2026 NEHRP Provisions.

Following this, the period of a representative design model (limited to the LFRS) is determined, considering the target seismic drift and stability requirements (ASCE 7-22 Section 12.8.7). This involves constructing a simple multi-degree-of-freedom (MDOF) model that reflects the system's mass and stiffness characteristics. For instance, moment frames tend to be more shear-dominated, whereas walls and braced frames are more flexure-dominated. This approach is based on a method developed by Miranda (1999) and Miranda and Reyes (2002) but utilizes matrix structural analysis with mass and stiffness matrices rather than purely analytical equations; it also incorporates the ability to model rotational flexibility at the base.

Starting from very low stiffness, the stiffness matrix is systematically scaled (i.e., increased) until the model achieves the target drift or less while satisfying stability requirements. Generally, modal response spectrum analysis (MRSA) is used to generate structural properties for modern code-compliant buildings that are taller than four stories and located in high- or very high-seismic areas. For other cases, the equivalent lateral force (ELF) procedure is used. Wind drift checks can be included in this step but were omitted for this study.

Next, the expected strength and stiffness of the LFRS are determined, accounting for overstrength. These properties vary depending on the LFRS type and building height and are calibrated using results from OpenSees models and engineering judgment. An additional optional check can be performed to ensure compatibility between strength and stiffness. If the stiffness is found to be too high or low in relation to the strength and yield drift, it is adjusted to a reasonable level.

The final estimates of the first three periods and mode shapes of the building are determined by performing an eigen analysis with the stiffness matrix and mass matrix. The final estimate of the ultimate base shear strength is determined from design strength and the expected overstrength.

2.4.3. Story Drift Ratio

The Moment Frame SRPE estimates peak story drift ratio at each story, accounting for the first three mode shapes and periods of the building and its peak strength. First, peak roof drift ratio is estimated using a method that is similar to the ASCE 41 (ASCE, 2023) method for target roof displacement (Section 7.4.3.3.2), but with factors calibrated directly to the OpenSees model results; it depends on the fundamental building period, modal participation factor, spectral acceleration, and correction factors for nonlinear behavior. Second, linear modal analysis is performed using the first three modes, and the results are scaled to reproduce the roof drift from the first step. If the spectral acceleration demand is large enough to cause yielding in the structure, then the story drifts are adjusted to account for nonlinear demands. Nonlinear demands are adjusted using an intensity factor S = Sa/(Vmax/W), where Sa is the first-mode spectral acceleration and (Vmax/W) denotes the normalized peak strength of the building based on expected properties. Larger values of S (i.e., more damage) result in more drift concentration in the lower stories. The way in which drifts localize as S increases is calibrated to nonlinear modeling results and depends on the building height (i.e., number of stories). An example calibration for a 12-story RC special moment frame model is shown in Figure 14. The solid lines represent the median peak drift profile from nonlinear time history analysis (NRHA) compared to SRPE response shown in thicker dashed lines. The dotted lines show the elastic response profile before adjusting for nonlinear behavior.

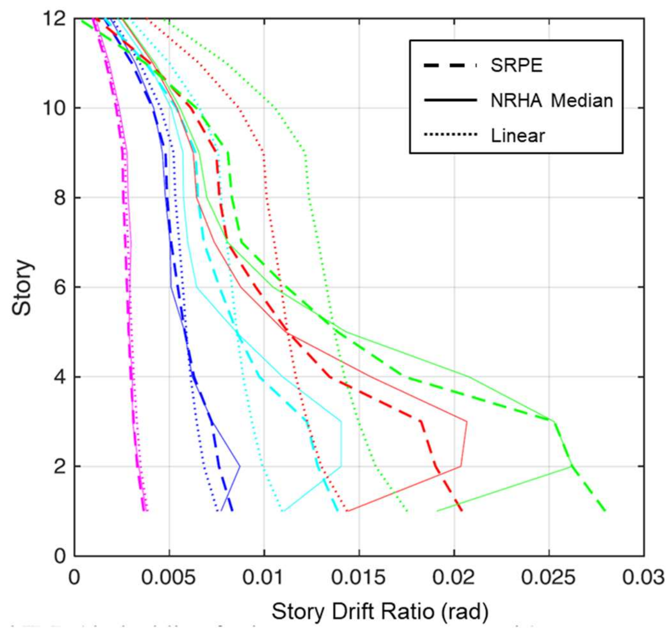

Figure 14. Comparison of SRPE (dashed) and median NRHA (solid) story drift ratio response for a 12-story RC special moment frame. Note, dotted lines represent predicted linear response prior to adjustment for nonlinear behavior. Figure adapted from Cook et al. (2018).

2.4.4. Peak Floor Acceleration

Peak floor acceleration (PFA) is computed based on spectral acceleration, building strength, and the first three modal periods and shapes of the building. First, elastic PFA is computed using modal time-history analysis of the FEMA P-695 far-field record set, scaled to the intensity of interest. Then, if the spectral acceleration demand is large enough to cause yielding, PFA is adjusted using the intensity factor $S = S_a/(V_{max}/W)$. The amount of reduction of the response depends on how high the story is above the ground, because damage in the lower stories "isolates" the upper stories from acceleration input. An example calibration for a 12-story RC special moment frame model is shown in Figure 15. The solid lines represent the median PFA profile from NRHA compared to the SRPE response shown in thicker dashed lines. The dotted lines show the elastic response profile before adjusting for nonlinear behavior. Note that the largest intensity shaking (green lines) has significant reductions in PFA at upper stories due to damage in the lower stories.

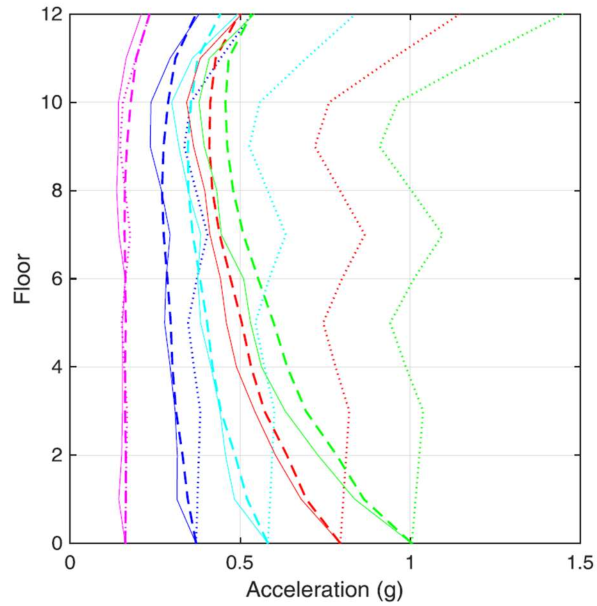

Figure 15. Comparison of SRPE (dashed) and median NRHA (solid) peak floor acceleration response for a 12-story RC special moment frame. Dotted lines represent predicted linear response before adjustment for nonlinear behavior. Figure adapted from Cook et al. (2018).

2.4.5. Treatment of Residual Drift Ratio

The estimation of residual drift and the probability that a structure will require demolition or straightening is typically performed in FEMA P-58/ATC-138 analyses. However, for the PHMF system, residual drift is not included in the analyses, reflecting the self-centering capabilities of hybrid connections with unbonded PT tendons. This modeled behavior is supported by prior experimental research and is one of the system's advantages over traditional monolithic (cast-in-place) RC moment frames (Kurama et al. 2018). A summary of the observed experimental residual drifts from all the test specimens considered for fragility development (refer back to Table 3) is provided in Figure 16. The figure shows that specimens can be loaded to very large drift ratios, on the order of 5% to 7%, without any residual drift being observed upon unloading. One test shows a very small residual drift (0.04%) due to concrete spalling being wedged within the connection gap, yet this amount of residual drift can be considered negligible. These observations, in combination with assessing the PHMF system at the FRE_R, which is less intense than the DE used for life-safety design, support the assumption of neglecting residual drift for the current study.

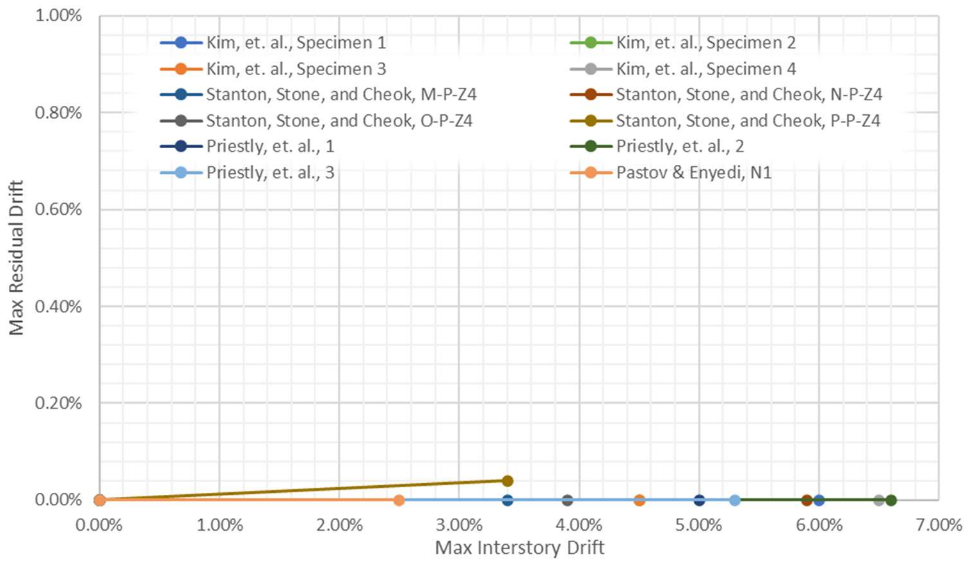

Figure 16. Reported residual drift ratios following testing of precast hybrid moment frames and subassemblies (Fitzgerald et al. 2016).

3. RESULTS

The tables and plots below show the R_{fr} and Δ_{afr} envelopes for each combination of performance group variants. This design envelope identifies the possible design value combinations where all performance groups satisfy both the max and mean analysis criteria. Results are provided separately for both FRC A/B/C acceptance criteria in Section 3.1 and FRC D acceptance criteria in Section 3.2. Additional figures that illustrate general system performance in terms of structural response, controlling component damage, and controlling design features are provided in Section 3.3. Full details on the performance of individual archetypes are provided in the attached supplementary materials.

3.1. FRC A/B/C Analysis Results

Table 8 – R_{fr} values across various allowable drift limits required to satisfy the FRC A/B/C structural performance acceptance criteria for each performance group. Analysis results assume increased strength requirements impact building stiffness.

Performance Group	Criteria	Δ_{afr} 0.005	0.0075	0.01	0.0125	0.015	0.0175	0.02
PG1-PHMF	Max[1]	8	8	8	8	6.5	4.5	4.5
PG2-PHMF		8	8	8	7.5	3.5	3	3
PG3-PHMF		8	8	8	8	8	4.5	3.5
PG1-PHMF	Mean[1]	8	8	8	7	5.5	5	4.5
PG2-PHMF		8	8	7.5	4	2.5	2.5	2.5
PG3-PHMF		8	8	8	8	4	3	3
	Envelope	8	8	7.5	4.0	2.5	2.5	2.5

[1]In each performance group, the combination of R_{fr} and Δ_{afr} is deemed to be acceptable if the mean P[SCSD] is less than 10%, and the maximum P[SCSD] across all archetypes in the performance group is less than 20%.

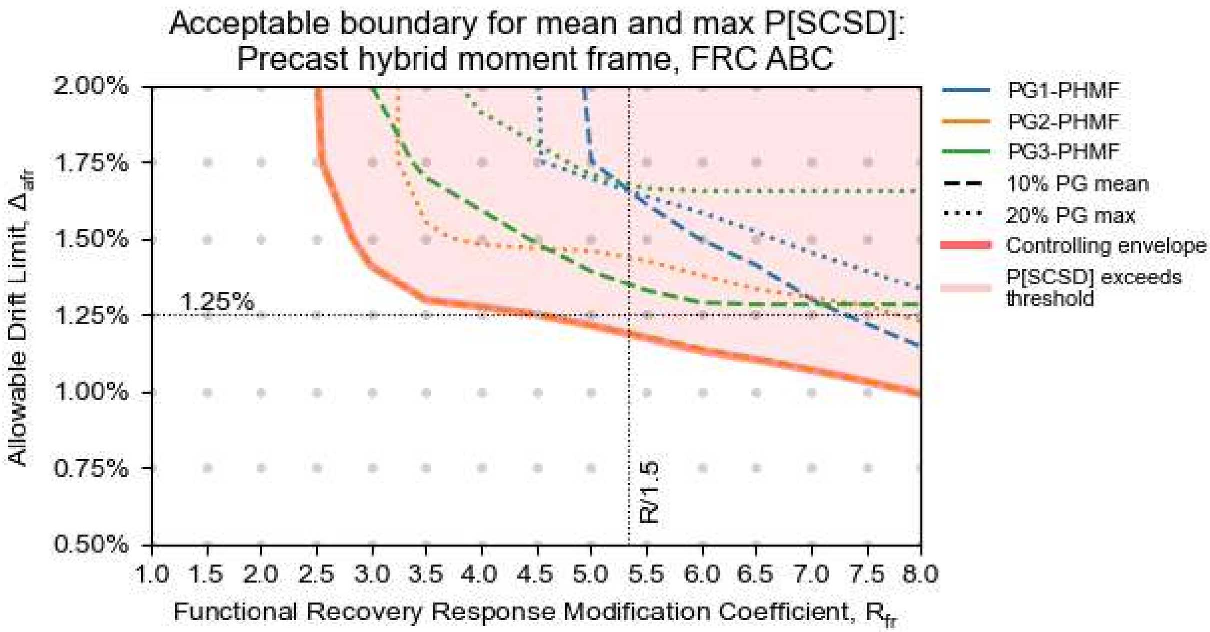

Figure 17 – Combination of R_{fr} and Δ_{afr} values required to satisfy the FRC A/B/C structural performance acceptance criteria for each performance group. Analysis results assume increased strength requirements impact building stiffness.

3.2. FRC D Analysis Results

Table 9 – R_{fr} values across various allowable drift limits required to satisfy the FRC D structural performance acceptance criteria for each performance group. Analysis results assume increased strength requirements impact building stiffness.

Performance Group	Criteria	Δ_{afr}						
		0.005	0.0075	0.01	0.0125	0.015	0.0175	0.02
PG1-PHMF	Max[1]	8	8	8	8	7.5	5.5	5
PG2-PHMF		8	8	8	8	6	3.5	3.5
PG3-PHMF		8	8	8	8	8	8	4.5
PG1-PHMF	Mean[1]	8	8	8	8	7	6	5.5
PG2-PHMF		8	8	8	6.5	3.5	3	3
PG3-PHMF		8	8	8	8	8	8	3.5
	Envelope	8	8	8	6.5	3.5	3	3

[1]In each performance group, the combination of R_{fr} and Δ_{afr} is deemed to be acceptable if the mean P[SCSD] is less than 15%, and the maximum P[SCSD] across all archetypes in the performance group is less than 25%.

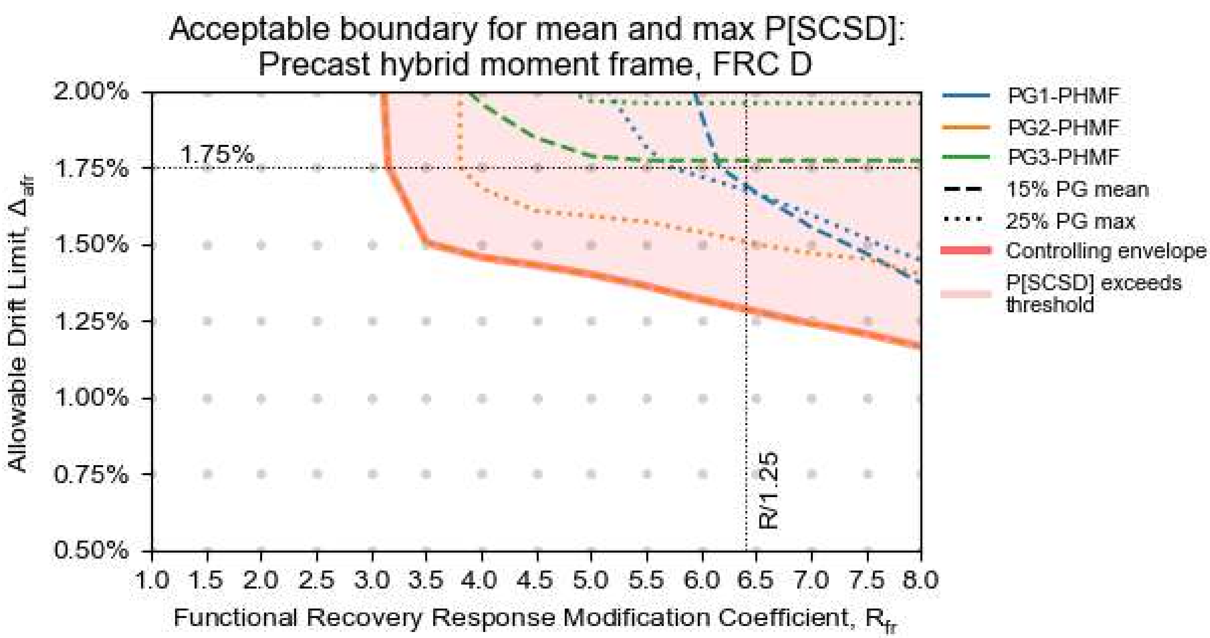

Figure 18 – Combination of R_{fr} and Δ_{afr} values required to satisfy the FRC D structural performance acceptance criteria for each performance group. Analysis results assume increased strength requirements impact building stiffness.

3.3. System Response

The figures below provide detailed insights into the general response and performance outcomes of the models making up each performance group. Figure 19 shows how design drift (Δ_{afr}) relates to median realized drift (x-axis), and how realized drift relates to P[SCSD] (y-axis). The median realized drift is the median peak story drift, in a given story, from all the realizations of peak story drift (~2,000) simulated as part of the FEMA P-58 Monte Carlo assessment. Figure 20 and Figure 21 further break down the contributions of SCDS by structural component type, and shows that residual drifts are dominant in many of the performance results for BRBF buildings. Finally, Figure 22 shows when the building design transitions from strength-controlled to stiffness-controlled for various R_{fr} and Δ_{afr} combinations. All results presented in this section are general to the response of the system and not specific to Functional Recovery Category.

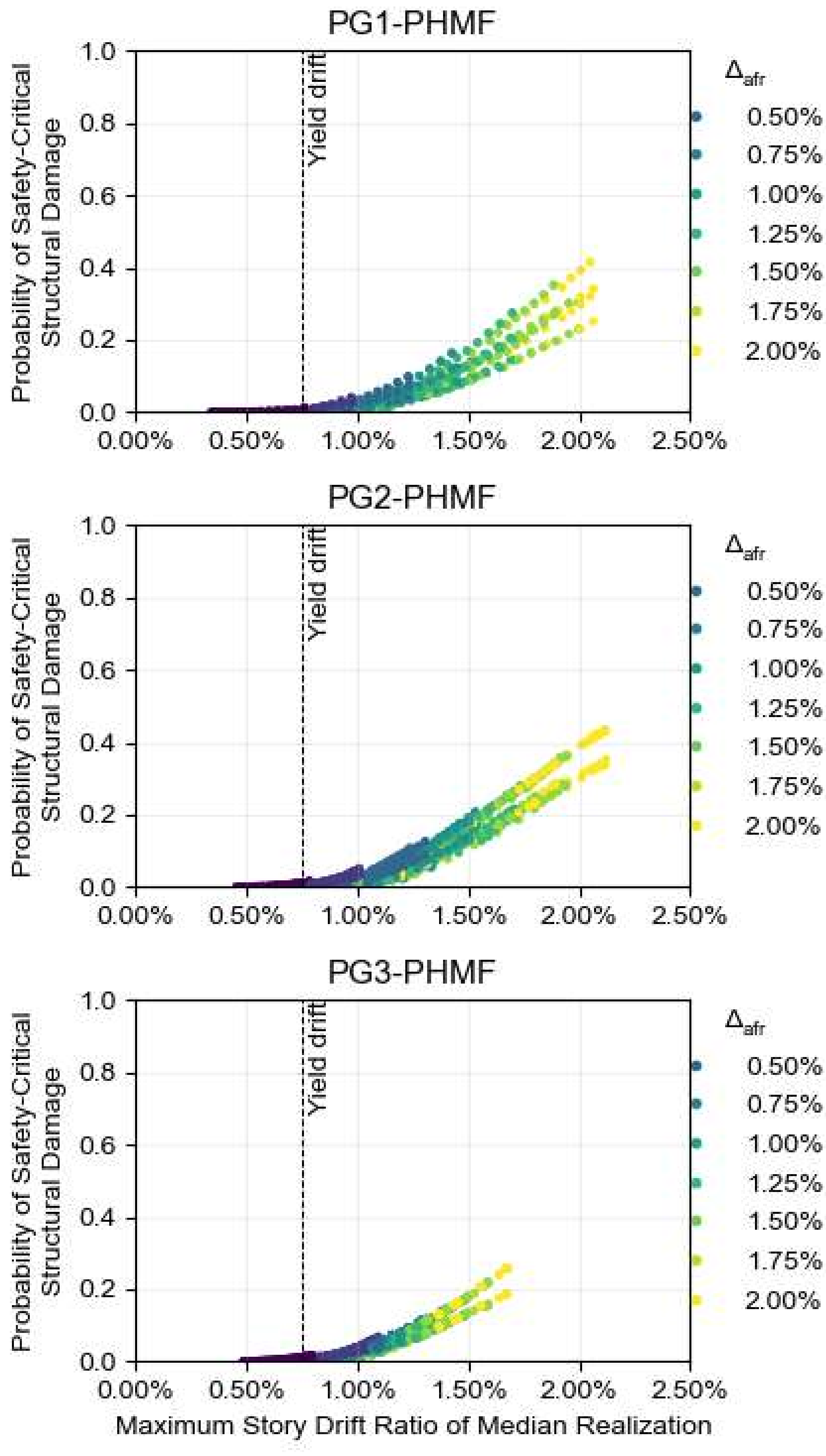

Figure 19 - Relationship between peak realized drift (median) and P[SCSD] for all archetypes.

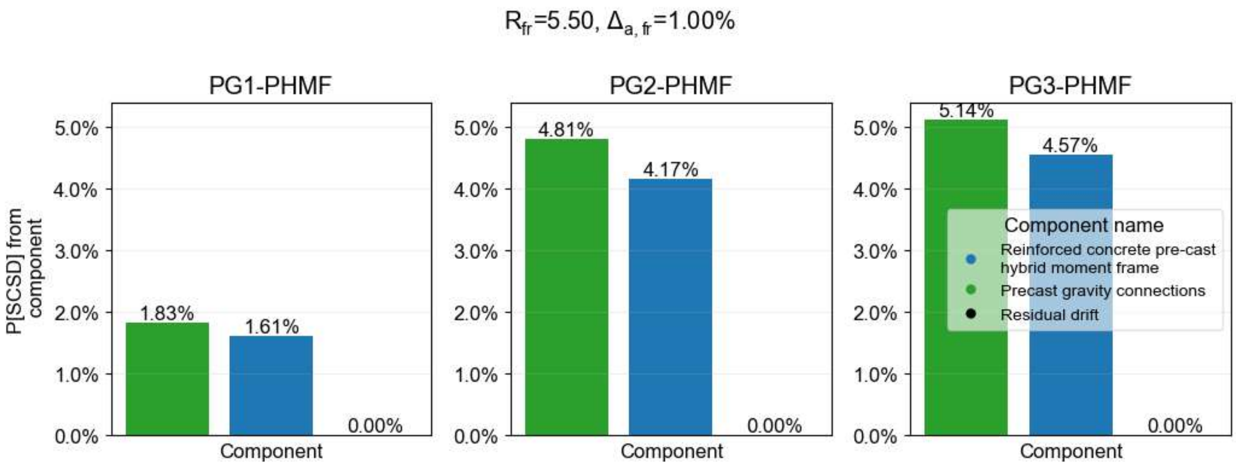

Figure 20 – Component damage contribution to P[SCSD] for each performance group at the recommended design points for FRC ABC

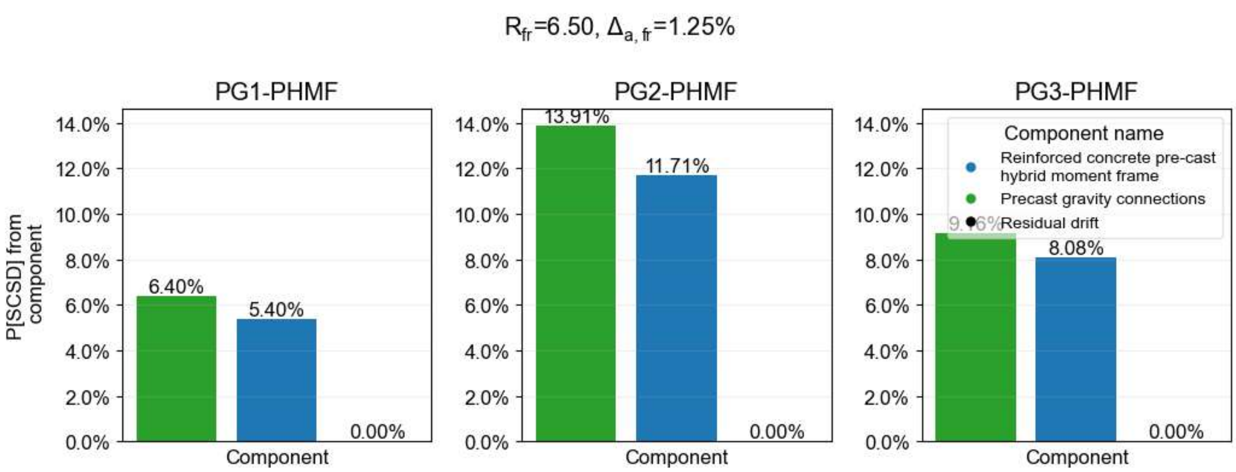

Figure 21 – Component damage contribution to P[SCSD] for each performance group at the recommended design points for FRC D

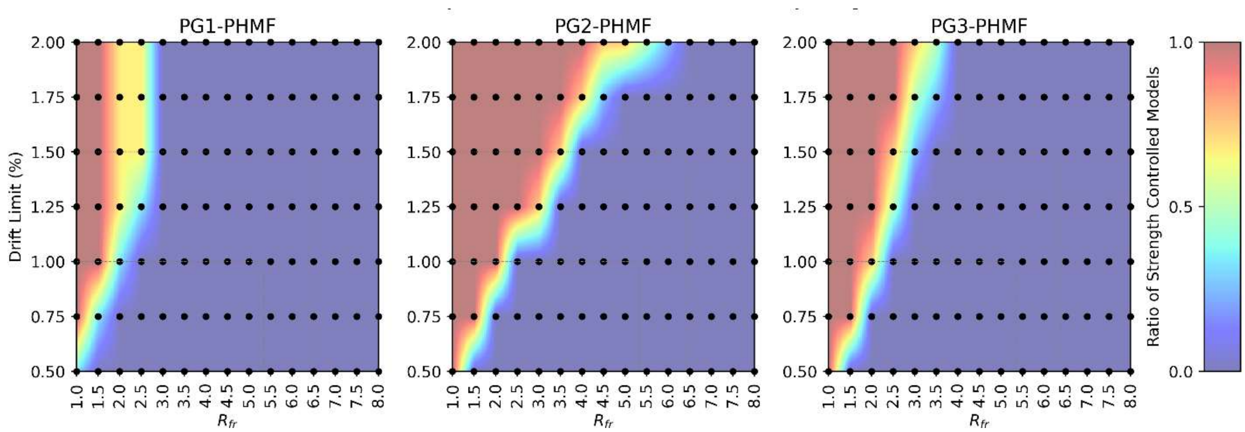

Figure 22 – Average influence of strength on building stiffness for various design requirement combinations assessed. Red coloring indicates that 100% of the models at this design point are controlled by strength requirements (e.g., tightening drift limits by one increment will not change performance). Alternately, blue coloring indicates that 100% of the models at this design point are controlled by stiffness requirements.

3.4. Validation of Peak Floor Acceleration Demand Estimates

The prequalification method documented in the 2026 NEHRP Section A.8.3.6 requires that the peak floor acceleration demands be evaluated for all of the structural system archetype design cases, to ensure that the Section A.10.6 peak floor acceleration adequately reflects the actual peak floor acceleration values observed in the nonlinear response-history analysis results. If the peak floor acceleration demands exceed the acceptable limits of Section A.8.3.6, the recommended $R_{\mu fr}$ value is reduced from the baseline $R_{\mu fr}$ value to adequately adjust the peak floor acceleration demands when using the Section A.10.6 equation. The baseline $R_{\mu fr}$ values are calculated in accordance with Section 13.3.1.2 with the following modifications:

1. R_{fr} and Ω_{0fr} are used in lieu of R and Ω_0
2. The value of I_e is taken as 1.0.
3. The lower limit on $R_{\mu fr}$ of 1.3 in Equation 13.3-6 does not apply.

The recommended R_{ufr} values are determined by checking for compliance with the following two criteria:

1. The ratio of the median peak floor acceleration from analysis averaging across all structural levels to the seismic floor acceleration determined in accordance with Section A.10.7 averaged across all structural levels is computed. The average of this ratio across all archetypes within a performance group shall not exceed 1.0.
2. The ratio of the largest peak floor acceleration from analysis at any level to the largest seismic floor acceleration determined in accordance with Section A.10.7 at any structural level is computed. The average of this ratio across all archetypes within a performance group shall not exceed 1.2.

The Section A.8.3.6 evaluation was completed, resulting in the following $R_{\mu fr}$ requirements:

- $R_{\mu fr}$ = 1.40 is required for FRC A/B/C (based on design using R_{fr} = 5.5 and Δ_{afr} = 1.00%), the same as the baseline value, therefore, no change is required.
- $R_{\mu fr}$ = 1.55 is required for FRC D (based on design using R_{fr} = 6.5 and Δ_{afr} = 1.25%), the same as the baseline value, therefore, no change is required.

4. CONCLUSIONS

This report documents the quantification of the functional recovery seismic performance factors for the Precast Hybrid Moment Frame (PHMF) system in accordance with the proposed Section A.8.3.6 procedures of the 2026 National Earthquake Hazards Reduction Program (NEHRP) Provisions. The recommended functional recovery seismic performance factors for the PHMF are summarized in Table 10. These include the functional recovery response modification coefficient, R_{fr}, the functional recovery allowable story drift limit, $\Delta_{afr.}$, and the functional recovery structural ductility reduction factor, $R_{\mu fr}$, for estimation of peak floor accelerations.

Results from the assessment showed that the functional recovery performance factors for PHMFs were primarily governed by damage to the precast primary gravity connections in the mid-rise performance groups, with design criteria governed by the 10% mean acceptance criteria.

In selecting the performance factors, preference was given to performance factor combinations with tighter drift limits and R_{fr} at or near the judgement-based limit. This approach was taken because safety-critical structural damage results from excessive displacement, and enforcing stricter drift limits is the more direct way to control displacements. For PHMF with fixed beam-to-column connections, a drift limit of Δ_{afr} equal to 1.00% and 1.25% achieves the performance goals for FRC A/B/C and FRC D, respectively, without needing to reduce R_{fr} below the judgment-based limits of R/1.5 = 5.5 and R/1.25 = 6.5, respectively.

In comparison with functional recovery seismic performance factors quantified for cast-in-place reinforced concrete moment frames (R_{fr} of 4.5 and Δ_{afr} of 1.0% for FRC A/B/C and R_{fr} of 5.5 and Δ_{afr} of 1.0% for FRC D), PHMF system performance showed lower probabilities of SCSD due to larger moment frame connection deformation capacities and lack of post-earthquake residual drift issues, resulting in less restrictive recommended seismic performance factors.

Table 10. Summary of functional recovery seismic performance factors for PHMF lateral systems complying with ACI 550.3 (ACI, 2022).

	FRC A/B/C			**FRC D**		
	R_{fr}	**Δ_{afr}**	**$R_{\mu fr}$†**	**R_{fr}**	**Δ_{afr}**	**$R_{\mu fr}$†**
Analysis results	7.5	1.00%	--	6.5	1.25%	--
Judgment-based upper limit	5.5	1.25%	--	6.5	1.75%	--
Recommendation – PHMF	**5.5**	**1.00%**	**1.40***	**6.5**	**1.25%**	**1.55***

†$R_{\mu fr}$ is only calculated for the recommended seismic performance factors

**Equivalent to the baseline value calculated using R_{fr}*

SUPPLEMENTARY MATERIAL

Two supplementary files are attached to this Prequalification Report that provide additional detailed information on the structural response and ATC-138 outcomes from individual archetype models and performance groups, as well as performance outcomes from the independent-strength-and-stiffness check discussed in the body of the report. The general description of the content contained in each file is provided below to assist with navigation and comprehension of detailed results.

- **Analysis Report Tables**
  (*"SupplementalData_AnalysisReportTables_PHMF_v1_10c_final.xls"*)
  - Contains detailed analysis outcomes for each archetype model assessed, including results for FRC A/B/C and FRC D.
  - "Summary" tab provides a summary of the controlling design values and other response metrics for each archetype.
  - "All Runs" tab provides response and performance outcomes for all combinations of model runs for each archetype.
- **Archetype Performance Plots**
  (*"SupplementalData_ArchtypePerformancePlotsAppendix_PCHMF_v1_10c_final.pdf"*)
  - Provides visualizations of analysis outcomes similar to the figures in the report, but for the independent-strength-and-stiffness check.
  - Provides visualizations of analysis outcomes similar to the figures in the report, but for individual archetype models.
  - Provide peak transient drift, residual drift, and peak floor acceleration response profiles for each archetype model.

REFERENCES

ACI. (2019a). "Building Code (and Commentary) Requirements for Structural Concrete," *ACI 318-19/ACI 318R-19*, American Concrete Institute, Farmington Hills, MI.

ACI. (2019b). "Acceptance Criteria for Moment Frames Based on Structural Testing and Commentary," *ACI 374.1-05(19)*, Reapproved 2019, American Concrete Institute, Farmington Hills, MI.

ACI. (2022). "Design Specification for Unbonded Post-Tensioned Precast Concrete Special Moment Frames Satisfying ACI 374.1 (ACI 550.3-13) and Commentary, *ACI 550.3-13(22)*, Reapproved 2022, American Concrete Institute, Farmington Hills, MI.

Almeter, E. (2017). "Report for Phase I – Structural Response Prediction Method for CoreBrace Buckling Restrained Brace Frame Buildings," Prepared by Haselton Baker Risk Group for CoreBrace, LLC, West Jordan, UT.

Almeter, E., Wade, K.F., Haselton, C.B., Saxey, B. (2018). "Rapid Risk Assessment of Buckling Restrained Braced Frames, With Focus on Residual Drifts," *Proceedings of the 11th U.S. National Conference on Earthquake Engineering* (11NCEE), Los Angeles, CA.

ASCE. (2022). "Minimum Design Loads and Associated Criteria for Buildings and Other Structures," *ASCE/SEI 7-22*, American Society of Civil Engineers, Reston, VA.

ATC. (2021). "Seismic Performance Assessment of Buildings: Volume 8 – Methodology for Assessment of Functional Recovery Time, *ATC-138-3*, Preliminary report for FEMA P-58-8, Prepared by the Applied Technology Council for the Federal Emergency Management Agency, Washington, DC.

Blowes, K., Molina Hutt, C., Zimmerman, R., Cook, D.T., Almeter, E., Haselton, C.B. (in press). "Limiting Safety-Critical Structural Damage in Recovery-Based Seismic Design Provisions," *Earthquake Spectra*.

Cook, D., Wade, K., Haselton, C., Baker, J. W., & DeBock, D. J. (2018). A structural response prediction engine to support advanced seismic risk assessment. In *Eleventh US national conference on earthquake engineering, Los Angeles, CA*.

Corney, S.R., Henry, R.S., Ingham, J.M. (2014). "Performance of precast concrete floor systems during the 2010/2011 Canterbury earthquake series," *Magazine of Concrete Research*, **66**(11): 563-575.

DeBock, D., Manousakis, I.V., Deierlein, G.G., Zsarnóczay, A. (2024). "Updated Model and Criteria for Residual Drift," *FEMA P-58/BD-3.7.26*, Background documentation for the ATC-138/FEMA P-58 Project, Submitted to the Applied Technology Council, Prepared for the Federal Emergency Management Agency, Washington, DC.

FEMA. (2009). “Quantification of Building Seismic Performance Factors,” *FEMA P695*, Prepared by the Applied Technology Council for the Federal Emergency Management Agency, Washington, DC.

FEMA. (2018). “Seismic Performance Assessment of Buildings: Volume 1 - Methodology,” *FEMA P-58-1*, 2nd Edition, Prepared by the Applied Technology Council for the Federal Emergency Management Agency, Washington, DC.

FEMA. (2018b). “Seismic Performance Assessment of Buildings: Volume 2 – Implementation Guide,” *FEMA P-58-2*, 2nd Edition, Prepared by the Applied Technology Council for the Federal Emergency Management Agency, Washington, DC.

fib (Fédération internationale du béton). (2003). “Seismic design of precast concrete building structures,” *fib Bulletin 27*, Lausanne, Switzerland.

Fitzgerald, K., Haselton, C., Baker, J., Cook, D. (2016). “Fragility Functions for the Precast Hybrid Moment Frame System,” Prepared by Haselton Baker Risk Group for Clark Pacific, West Sacramento, CA.

Ghosh, S.K., Cleland, N.M., Naito, C.J. (2017). “Seismic Design of Precast Concrete Diaphragms: A Guide for Practicing Engineers,” *NIST GCR 17-917-47*, ATC for NIST, Gaithersburg, MD.

Ghosh, S.K. (2022). "Seismic design force level for precast concrete diaphragms," *PCI Journal*, **67**(2): 20-33.

Gogus, A., Wallace, J. (2008). “Fragility Curves for Slab-Column Connections,” *FEMA P-58/BD-3.8.7*, Background document for the FEMA P-58 project, Submitted to the Applied Technology Council for the Federal Emergency Management Agency, Washington, DC.

Hare, J., Fenwick, R.C., Bull, D., Built, R. (2009). “Precast Double Tee Support Systems,” *Journal of the Structural Engineering Society New Zealand,* **22**(1): 10-44.

Hare, J., Bull, D., Elwood, K., Henry R., Brooke, N. (2018). “Precast Double Tee Support System – 10 Years On,” *Proceedings of the 2018 Concrete New Zealand Conference*, Hamilton, New Zealand.

Haselton Baker Risk Group (2025). Seismic Performance Prediction Program (SP3).

Henry, R.S., Dizhur, D., Elwood, K.J., Hare, J., Brundson, D. (2017). “Damage to Concrete Buildings with Precast Floor During the 2016 Kaikoura Earthquake,” *Bulletin of the NZSEE*, **50**(2): 174-186.

Iverson, J.K., Hawkins, N.M. (1994). “Performance of Precast/Prestressed Concrete Buildings During Northridge Earthquake,” *PCI Journal*, **39**(2): 38-55.

Kam, W.Y., Pampanin, S., Dhakal, R., Gavin, H.P., Roeder, C. (2010). "Seismic Performance of Reinforced Concrete Buildings in the September 2010 Darfield (Canterbury) Earthquake, *Bulletin of the NZSEE*, **43**(4): 340-350.

Kam, W.Y., Pampanin, S., Elwood, K. (2011). "Seismic Performance of Reinforced Concrete Buildings in the 22 February Christchurch (Lyttleton) Earthquake, *Bulletin of the NZSEE*, **44**(4): 239-278.

Kim, J., et. al. (2004), "Cyclic Load Testing of Precast Hybrid Moment Frame Connections." *13th World Conference on Earthquake Engineering*, Vancouver, Canada.

Kurama, Y. C., Sritharan, S., Fleischman, R. B., Restrepo, J. I., Henry, R. S., Cleland, N. M., Ghosh, S. K., & Bonelli, P. (2018). Seismic-resistant precast concrete structures: State of the art. *Journal of Structural Engineering, 144*(4), Article 03118001. https://doi.org/10.1061/(ASCE)ST.1943-541X.0001972

MBIE. (2018). "Warning Against the Use of Loop Bar Details in Flange-Hung Double-Tee Precast Concrete Floor Units that do not Comply with NZS 3101 (Warning 2018/01)," Ministry of Business, Innovation, and Employment, Wellington, New Zealand.

Miranda, E. (1999). "Approximate seismic lateral deformation demands in multistory buildings," *Journal of Structural Engineering*, **125**(4): 417-425.

Miranda, E., Reyes, C.J. (2002). "Approximate lateral drift demands in multistory buildings with nonuniform stiffness," *Journal of Structural Engineering*, **128**(7): 840-849.

McKenna, F., Scott, M.H., Fenves, G.L. (2010). "Nonlinear Finite-Element Analysis Software Architecture using Object Composition," *Journal of Computing in Civil Engineering*, **24**(1): 95-107.

Pastrav, M. and Enyedi, C. (2012). Hybrid Moment Frame Joints Subjected to Seismic Type Loading. *15th World Conference on Earthquake Engineering*. Lisbon, 2012.

PCI (1988). "Design and Typical Details of Connections for Precast and Prestressed Concrete," *PCI MNL 123-88*, Prestressed Concrete Institute, Chicago, IL.

Priestley, M. J. N., Sritharan, S., Conley, J. R., & Pampanin, S. (1999). Preliminary results and conclusions from the PRESSS five-story precast concrete test building. PCI Journal, 44(6), 42–67. https://doi.org/10.15554/pcij.11011999.42.67

Roskelley, B. (2025). Discussion on typical details of precast gravity framing, *Personal communication*, Blake Roskelley, Senior Preconstruction Manager, Clark Pacific.

Stanton, J., Stone, W. C., & Cheok, G. S. (1997). A hybrid reinforced precast frame for seismic regions. PCI Journal, 42(2), 20-32. https://doi.org/10.15554/pcij.03011997.20.23

Todd, D., Carino, N., Chung, R.M., Lew, H.S., Taylor, A.W., Walton, W.D., Cooper, J.D., Nimis, R. (1994). "1994 Northridge Earthquake – Performance of Structures, Lifelines, and Fire

Protection Systems," *NIST Special Publication 862*, National Institute of Standards and Technology, Gaithersburg, MD.